A Mounting Configuration for Efficient Third Harmonic Conversion of KDP Crystals with Large Aperture

Jia Kai[1] Xiong Zhao[2] Yang Chuang[1] Gao Heng[1] Xu Pan[3] Yang Feng[1] Zhang Bin[3]

[1] *Southwest Institute of Technical Physics, Chengdu, Sichuan* 610041, *China*
[2] *Research Center of Laser Fusion, China Academy of Engineering Physics, Mianyang, Sichuan* 621900, *China*
[3] *College of Electronics and Information Engineering, Sichuan University, Chengdu, Sichuan* 610065, *China*

Abstract A mounting configuration is presented to solve the loss of the third harmonic generation (THG) efficiency due to the gravitational effects. The analysis result of finite element model shows that the loss of the THG efficiency is nearly absent due to the gravitational effects when the original surface profile of the KDP crystals and mounting configuration is an ideal plane. Meanwhile, numerical simulation calculations are performed to analyze the influence of fabrication errors on the THG efficiency. Furthermore, the machining requirements of the peripheral milling have been discussed. The loss of the THG efficiency is nearly same under the different departure angles. The mounting configuration with the random error is acceptable, but the convex error and concave error should be controlled below 5 μm to realize efficient third harmonic output.

Key words nonlinear optics; inertial confinement fusion; mounting configuration; third harmonic generation; gravitational sag; fabrication errors

OCIS codes 190.2640; 120.4610; 190.4360

大口径 KDP 晶体实现高效三倍频转换的新型支撑结构

贾 凯[1] 熊 召[2] 杨 闯[1] 高 恒[1] 徐 攀[3] 杨 峰[1] 张 彬[3]

[1]西南技术物理研究所，四川 成都 610041
[2]中国工程物理研究院激光聚变研究中心，四川 绵阳 621900；[3]四川大学电子信息学院，四川 成都 610065

摘要 提出了一种新型支撑结构以解决大口径晶体重力凹陷作用引起的三倍频转换效率损失问题。有限元分析结果表明：当 KDP 晶体及支撑结构均为理想平面时，重力作用导致的三倍频转换效率的损失量几乎为 0。同时，针对不同倾斜角度下的接触面加工误差对三倍频转换效率的影响进行了大量的数值模拟。计算结果表明：采用新型支撑结构，不同倾斜角度对三倍频转换效率的影响基本相同；支撑结构表面存在随机加工误差对三倍频转换效率的影响程度较小；而当支撑结构存在凸形或凹形加工误差时，加工误差容许值必须控制在 5 μm 范围内以实现高效三倍频输出。

关键词 非线性光学；惯性约束聚变；支撑结构；三次谐波；重力凹陷；加工误差

中图分类号 O437.1 **文献标识码** A **doi**：10.3788/CJL201340.0702004

1 Introduction

In the inertial confinement fusion (ICF) systems, the wavelength of the Nd:glass lasers will be converted from 1053 nm to 351 nm by frequency converters comprised of one block of the type I KDP crystal (doubler) and one block of the type II KDP crystal (mixer)[1-3]. Considering the input intensity and the limitation of damage threshold, the KDP crystals with large aperture (i.e., 430 mm × 430 mm) and low thickness (i.e., 12-mm-thick for the doubler and 9-mm-thick for the mixer) are widely used in high power laser systems. However, the surface profiles of these KDP crystals are very sensitive to the external factors (such as the gravitational sag, the mounting configuration and the

收稿日期：2012-12-26；**收到修改稿日期**：2013-01-26

作者简介：贾 凯(1985－)，男，博士研究生，主要从事高功率激光器及非线性光学工程应用等方面的研究。E-mail：jk200307@sina.com

导师简介：张 彬(1969－)，女，博士，教授，主要从事新固体激光技术和光束传变换与控制等方面的研究。E-mail：zhangbinff@sohu.com (通信联系人。)

mechanical vibration), leading to the obvious reduction of the third harmonic generation (THG) efficiency.

Frequency converters will be placed around the target chamber in several orientations departing from the vertical plane. Thus, the KDP crystals will be particularly sensitive to gravitational effect in ICF systems[4-8]. Consequently, several mounting configurations have been proposed in order to solve the loss of the THG efficiency due to the gravitational sag. These mounting configurations involve two methods to control the surface profiles of the KDP crystals[9-11]. The first method is to manage to maintain the original surface profile as much as possible; and the second is only to ensure that the detuning angular distribution along the extraordinary axis can be negligible. However, there are still some troubles in the existing mounting configurations. For example, the full edges support could not maintain the original surface profile very well[9], and the silicone fixed scheme could only ensure the detuning angular distribution for the doubler in order to avoid the damage of the silicone by the stimulated transverse Raman scattering[10].

In this paper, we present a mounting configuration based on the second method mentioned above to achieve efficient frequency conversion. The material of this mounting configuration is stainless steel which has a higher damage threshold than silicone. The effects of the gravitational sag on the THG efficiency by using the mounting configuration have been analyzed under three typical departure angles (i.e., 30°, 45° and 60°). Furthermore, the effects of the fabrication errors with different sizes (i.e., 5 μm, 10 μm and 15 μm) and types (i.e., random errors, convex errors and concave errors) on the surface profiles and the THG efficiency have been discussed in detail.

2 Design of the mounting configuration

2.1 Layout of the cascaded type I/II KDP crystals

The fundamental light is linearly polarized along the ordinary axis of the doubler. The 1ω and 2ω lights emerging from the doubler are linearly polarized along the extraordinary and ordinary axes of the mixer, respectively. Then 3ω light polarized along the extraordinary axis is finally generated by the nonlinear effect between the 1ω light and the 2ω light as shown in Fig. 1.

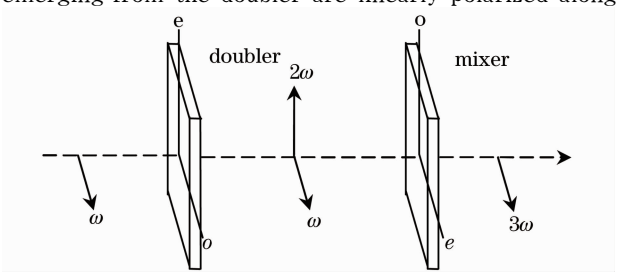

Fig. 1 Schematic of the cascaded type I/II KDP crystals

2.2 Design of the mounting configuration

Fig. 2 shows this mounting configuration including a rectangular metallic frame and some accessories (tablettings and small screws). The KDP crystals are held by their two vertical edges which are parallel to the extraordinary axis with the supporting stripes and the tablettings, and four small screws are fixed at each side of the KDP crystals with the equal interval. Because the dimension of the rectangular frame is slightly larger than the KDP crystals, the significance of these small screws is that the center of the KDP crystals could be aligned at that of the rectangular frame, besides, the ordinary axis of the doubler and the extraordinary axis of the mixer could be adjusted parallel to the polarized direction of the fundamental light.

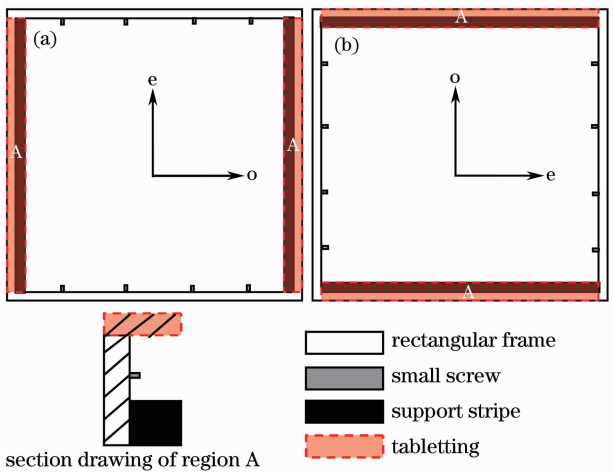

Fig. 2 Schematic of the mounting configuration. (a) Doubler; (b) mixer

2.3 Deformation model of the gravitational sag

The deformation model is performed by using the finite element software ANSYS[12]. For the boundary conditions, the surfaces of the mounting configuration abutting the KDP crystal could be treated as the contacted pairs in the finite element model and the deformation of the other surfaces is assumed to be negligible. The discretization of the KDP crystals is composed of 87 × 87 elements in the transverse plane and 5 elements in the thickness direction. The parameters used for the deformation model are as follows.

- KDP

Elastic stiffness (in units of GPa)

C_{11} = 71.2

C_{12} = −5.0

C_{13} = 14.1

C_{33} = 56.8

C_{44} = 12.6

C_{66} = 6.22

Density: ρ = 2.34 g/cm^3

- Stainless steel

Young's modulus E = 206 GPa

Poisson's ratio ν = 0.3

Density ρ = 7.39 g/cm^3

Fig. 3 and Fig. 4 show the deformation and the detuning angular distribution along the extraordinary axis of the KDP crystals when the departure angle is 45°.

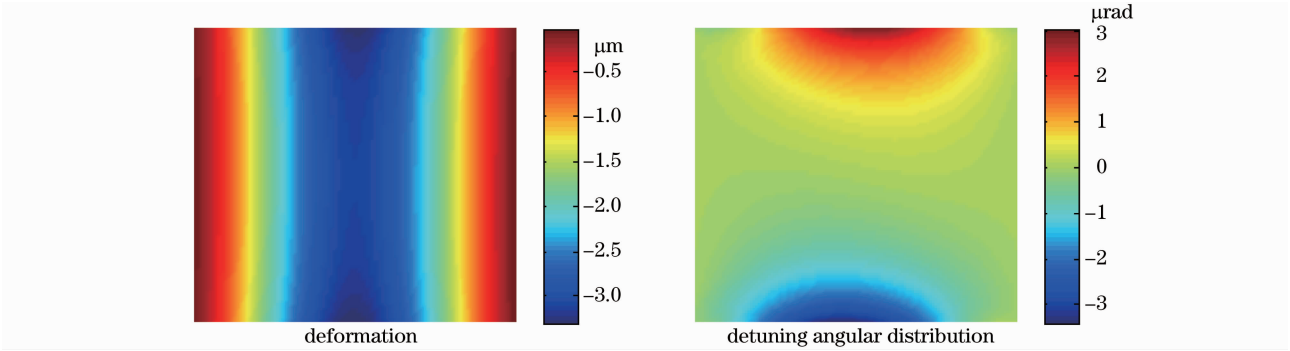

Fig. 3 Deformation and detuning angular distribution of the doubler

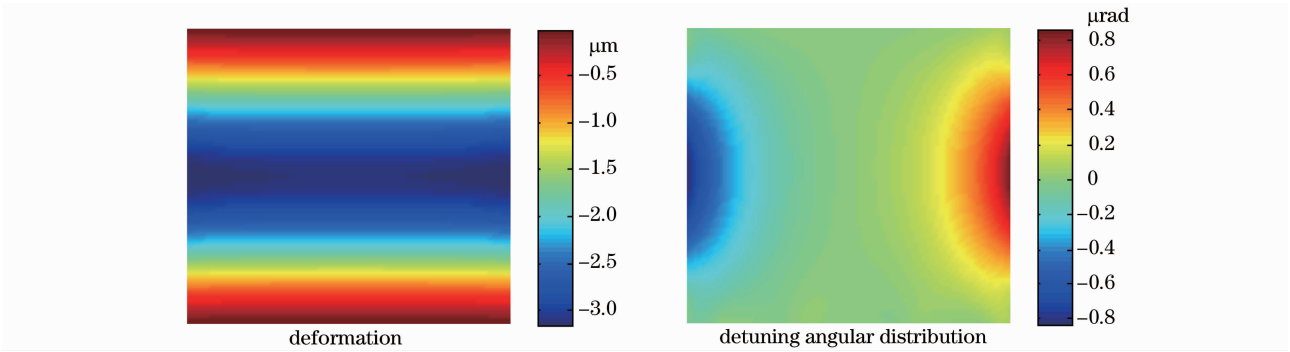

Fig. 4 Deformation and detuning angular distribution of the mixer

The peak-valley (PV) and the root mean square (RMS) values of the surface deformation can be expressed as

$$D_{\mathrm{PV}} = \psi_{\max} - \psi_{\min}, \tag{1}$$

$$D_{\mathrm{RMS}} = \sqrt{\sum_{n=1}^{N} (\psi_n - \psi_{\mathrm{ave}})^2 \Big/ (N-1)}, \tag{2}$$

where ψ is the amplitude of the surface deformation, N denotes the number of the sampling locations.

According to the equations (1) and (2), the D_{PV} and D_{RMS} values, as well as the average detuning angle along the extraordinary axis ($\Delta\theta_{\mathrm{ave}}$) of the KDP crystals have been calculated and listed in Table 1 (only the data in the clear aperture 410 mm × 410 mm are recorded).

Table 1 Deformation and detuning angle of the KDP crystals

KDP	Departure angle /(°)	D_{PV}/μm	D_{ems}/ μm	$\Delta\theta_{\mathrm{ave}}$ /μrad
Doubler	30	2.318	0.741	0.451
	45	3.256	1.049	0.566
	60	3.972	1.285	0.646
Mixer	30	2.206	0.738	0.110
	45	3.117	1.044	0.153
	60	3.816	1.278	0.188

Fig. 3 and Fig. 4 show that the surface profile of the KDP crystals exhibits several pinstripes along the extraordinary axis and the central region is sagged due to the gravitational effects. Besides, the detuning angular distribution caused by the crystal deformation almost tends to zero except in the small region near the two vertical edges which are parallel to the ordinary axis. Meanwhile, it can be shown from Table 1 that the D_{PV} value, the D_{RMS} value and $\Delta\theta_{\mathrm{ave}}$ of KDP crystals increase with the increment of the departure angle.

Generally speaking, the amplitude of the surface deformation is proportional to the width-thickness ratio, but the deformation of the doubler is larger than the mixer, as shown in Table 1. The reason is that the peripheral region of the KDP crystals is upwardly curved due to the gravitational effect and the tablettings would prevent the upward trend. The peripheral region of the mixer with the lower thickness would be upswept more obviously, so the reacting force of the tablettings exerted on the mixer is stronger than that on the doubler. Therefore, the deformation of the mixer is smaller than that of the doubler.

3 Loss of the THG efficiency

3.1 Conversion efficiency of the THG

For type I/II KDP angle-detuning method, the equations of harmonic conversion can be expressed as[13]

$$\begin{cases} \dfrac{\partial^2 E_1}{\partial x^2}+\dfrac{\partial^2 E_1}{\partial y^2}+\mathrm{i}2n_1\dfrac{\omega_1}{c}\left[\dfrac{\partial E_1}{\partial z}+\rho_\omega(\theta)\dfrac{\partial E_1}{\partial y}+a_1\dfrac{\partial E_1}{\partial t}\right]=-\dfrac{\omega_1^2}{c^2}\chi_{\mathrm{eff}}E_2^*E_3\exp(\mathrm{i}\Delta kz)-\mathrm{i}\dfrac{n_1\omega_1}{c}\alpha_1E_1 \\ \dfrac{\partial^2 E_2}{\partial x^2}+\dfrac{\partial^2 E_2}{\partial y^2}+\mathrm{i}2n_2\dfrac{\omega_2}{c}\left[\dfrac{\partial E_2}{\partial z}+\rho_{2\omega}(\theta)\dfrac{\partial E_2}{\partial y}+a_2\dfrac{\partial E_2}{\partial t}\right]=-\dfrac{\omega_2^2}{c^2}\chi_{\mathrm{eff}}E_1^*E_3\exp(\mathrm{i}\Delta kz)-\mathrm{i}\dfrac{n_2\omega_2}{c}\alpha_2E_2 \\ \dfrac{\partial^2 E_3}{\partial x^2}+\dfrac{\partial^2 E_3}{\partial y^2}+\mathrm{i}2n_3\dfrac{\omega_3}{c}\left[\dfrac{\partial E_3}{\partial z}+\rho_{3\omega}(\theta)\dfrac{\partial E_3}{\partial y}+a_3\dfrac{\partial E_3}{\partial t}\right]=-\dfrac{\omega_3^2}{c^2}\chi_{\mathrm{eff}}E_1E_2\exp(-\mathrm{i}\Delta kz)-\mathrm{i}\dfrac{n_3\omega_3}{c}\alpha_3E_3 \end{cases} \quad (3)$$

Here ρ is the walk-off coefficient of the extraordinary light; $a_j = 1/v_{gj} - 1/v_{g1}$ [$j = 1, 2, 3$ represent the fundamental light, the second harmonic generation (SHG) and the THG, respectively]; v_{gj} is group velocity; Δk is phase mismatch; c is the velocity of light in vacuum; α_j is the linear absorbing coefficient of KDP crystal.

For type I frequency doubling, $E_1 = E_2 = E_{1o}/2$ and E_{1o} is the ordinary light amplitude of the fundamental light; $E_3 = E_{2e}$, and E_{2e} is the extraordinary light amplitude of the SHG; $n_1 = n_2 = n_o$, and n_o represents the ordinary refractive index of the fundamental light; $n_3 = n_{2e}$, and n_{2e} is the extraordinary refractive index of the SHG; the effective nonlinear coefficient $\chi_{\mathrm{eff}} = -\chi^{(2)}\sin\theta\sin 2\Phi$, θ is the phase matching angle, the azimuth $\Phi = 45^\circ$ and the nonlinear coefficient $\chi^{(2)} = 7.8\times 10^{-13}$ m/V in equation (3).

And for type II frequency tripling, $E_1 = E_{1e}$, and E_{1e} is the extraordinary light amplitude of the fundamental light; $E_2 = E_{2o}$, and E_{2o} is the ordinary light amplitude of the SHG; $E_3 = E_{3e}$, and E_{3e} is the extraordinary light amplitude of the THG; $n_1 = n_e$ represents the extraordinary refractive index of the fundamental light; $n_2 = n_{2o}$ represents the ordinary refractive index of the SHG; $n_3 = n_{3e}$ represents the extraordinary refractive index of the THG; $\chi_{\mathrm{eff}} = \chi^{(2)}\sin\theta\cos 2\Phi$, and $\Phi = 0$.

For the sake of simplicity but without loss of practical interest, suppose that the spatial distribution of the fundamental light is the uniform plane wave. The expression of this fundamental light is given by

$$E(t) = \frac{E_0}{2}\exp[\mathrm{i}\omega t - \mathrm{i}kz] + c.c. \quad (4)$$

According to equations (3), (4) and the 4th Runge-Kutta equation, the relationship between the internal angular offset of the doubler and the THG efficiency is obtained and shown in Fig. 5.

Fig. 5 shows that if the largest THG efficiency could be achieved by type I/II KDP angle-detuning method, the doubler should have internal angular offsets of 180, 220, 230 μrad for the intensities of the fundamental light of 2, 3, 4 GW/cm², and the THG efficiencies are 83.27%, 88.77%, 90.95%, respectively.

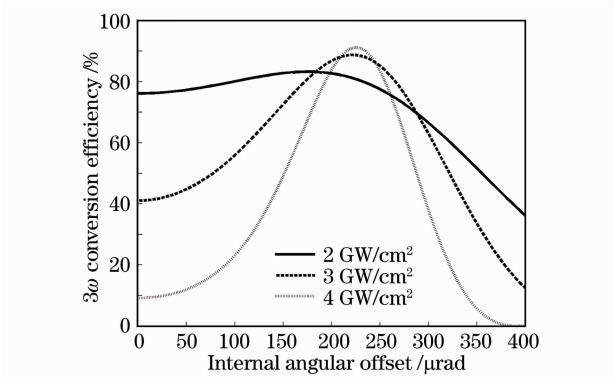

Fig. 5 THG efficiency of the plane wave

Because of the gravitational effects, the amplitudes of the surface deformation $\psi(x,y)$ are converted into a phase fluctuation in order to simulate the changes in the phase-matching direction:

$$\phi(x,y) = \frac{2\pi}{\lambda}\psi(x,y). \quad (5)$$

Then, equation (4) can be expressed as:

$$E(x,y,z,t) = \frac{E_0}{2}\exp[\mathrm{i}\omega t - \mathrm{i}kz + \mathrm{i}\phi(x,y)] + c.c. \quad (6)$$

When the original surface profile of the KDP crystals and mounting configuration is an ideal plane shown in Fig. 3 and Fig. 4, the maximal loss of the THG efficiency is only 0.02% due to the gravitational effects, indicating that this mounting configuration can maintain the THG efficiency very well when the surface profile of components is the ideal plane.

3.2 Loss of the THG efficiency due to fabrication errors

Peripheral milling of flexible components is a widely practiced manufacturing process in the machining industry[14-15]. The problem of machining is complicated, having periodically varying milling force exciting the flexible structure of the components both statically and dynamically, so fabrication errors are inevitable in this mounting configuration, especially in the support stripes and the tablettings.

Because each of the KDP crystals exhibits a different original surface profile and the debates focus on this mounting configuration, without loss of generality, the KDP crystals with an ideal surface and the mounting

configuration with fabrication errors have been analyzed to find out the relationship between fabrication errors and the loss of the THG efficiency. Fabrication errors can be divided into random errors, convex errors and concave errors by different machining types. Meanwhile, the sizes of fabrication errors analyzed are assumed to be 5, 10, 15 μm, respectively.

3.2.1 Condition of the random error

Fig. 6 and Fig. 7 show the deformation and the detuning angular distribution along the extraordinary axis of the KDP crystals when the departure angle is 45° and the fabrication error is a 10 μm random error. And the D_{PV} values, the D_{RMS} values, $\Delta\theta_{ave}$ and the loss of the THG efficiency are reported in Table 2.

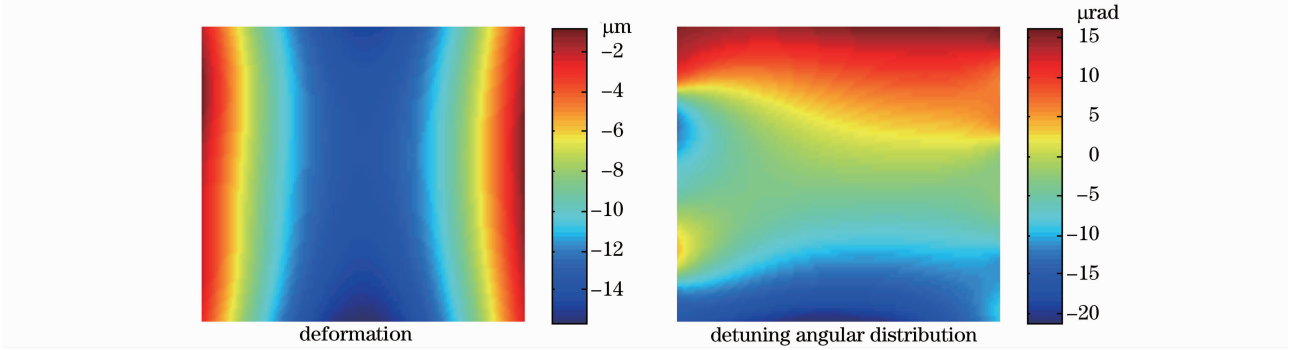

Fig. 6 Deformation and detuning angular distribution of the doubler under random errors

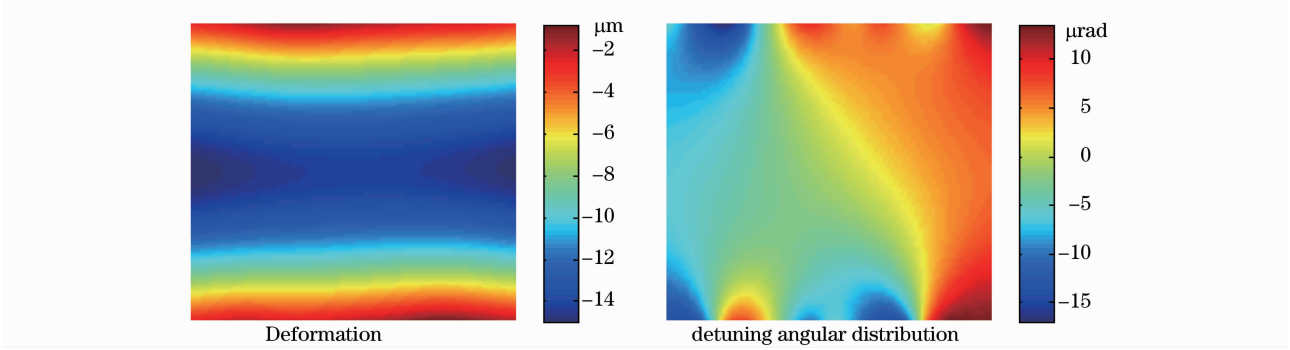

Fig. 7 Deformation and detuning angular distribution of the mixer under random errors

Table 2 Influence of random errors on frequency tripling

Departure angle /(°)	Random error /μm	KDP	D_{PV} /μm	D_{RMS} /μm	$\Delta\theta_{ave}$ /μrad	Loss of the THG efficiency /%		
						2 GW/cm²	3 GW/cm²	4 GW/cm²
30	5	Doubler	10.37	2.78	5.09	0.025	0.19	0.32
		Mixer	9.54	2.73	2.65			
	10	Doubler	10.99	2.85	6.56	0.046	0.30	0.56
		Mixer	10.23	2.78	4.32			
	15	Doubler	11.66	2.90	7.80	0.062	0.43	0.73
		Mixer	10.93	2.82	5.49			
45	5	Doubler	13.99	3.85	6.09	0.040	0.26	0.53
		Mixer	13.23	3.83	3.16			
	10	Doubler	14.80	3.95	7.60	0.065	0.39	0.82
		Mixer	14.10	3.95	4.85			
	15	Doubler	15.43	4.02	9.16	0.100	0.56	1.24
		Mixer	14.76	3.99	6.39			
60	5	Doubler	16.69	4.65	6.62	0.049	0.30	0.64
		Mixer	16.09	4.67	3.56			
	10	Doubler	17.70	4.80	8.41	0.083	0.47	1.06
		Mixer	17.12	4.86	5.18			
	15	Doubler	18.31	4.86	9.88	0.120	0.65	1.47
		Mixer	17.74	4.89	6.86			

Fig. 6 and Fig. 7 indicate that the restraint region of the mounting configuration with the random error becomes less, so the amplitudes of the deformation and the detuning angular distribution increase. But the surface profile is close to the gravitational deformation with the ideal plane. Table 2 shows that the mounting configuration with the random error is still used to achieve the efficient THG, and the maximal loss of the THG efficiency is less than 1.5%.

3.2.2 Condition of the convex error

Fig. 8 and Fig. 9 show the influence of the mounting configuration with a convex error on the KDP crystals when the departure angle is 45°. And the D_{PV} values, the D_{RMS} values, $\Delta\theta_{ave}$ and the loss of the THG efficiency are reported in Table 3.

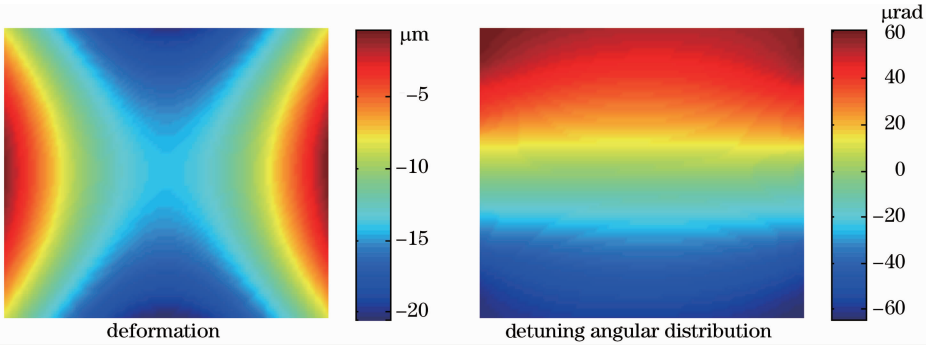

Fig. 8 Deformation and detuning angular distribution of the doubler under convex errors

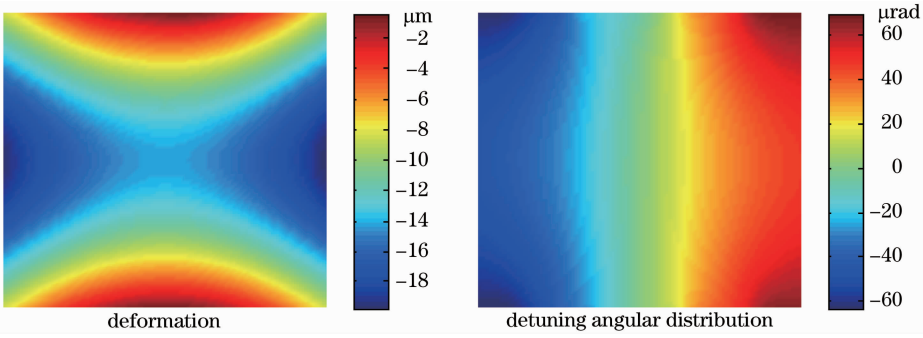

Fig. 9 Deformation and detuning angular distribution of the mixer under convex errors

Table 3 Influence of convex errors on frequency tripling

Departure angle /(°)	Convex error /μm	KDP	D_{PV} /μm	D_{RMS} /μm	$\Delta\theta_{ave}$ /μrad	Loss of the THG efficiency /%		
						2 GW/cm²	3 GW/cm²	4 GW/cm²
30	5	Doubler	13.05	3.04	18.84	0.49	2.09	5.71
		Mixer	11.93	2.88	16.57			
	10	Doubler	16.04	3.49	30.20	1.29	5.11	13.29
		Mixer	15.32	3.45	29.48			
	15	Doubler	18.19	3.88	38.73	2.13	8.07	20.10
		Mixer	16.97	3.73	39.29			
45	5	Doubler	16.74	4.11	19.93	0.56	2.35	6.43
		Mixer	15.69	3.98	16.93			
	10	Doubler	20.01	4.55	32.93	1.56	6.08	15.60
		Mixer	19.29	4.48	31.68			
	15	Doubler	22.74	4.98	43.78	2.71	10.11	24.39
		Mixer	21.51	4.79	43.46			
60	5	Doubler	19.53	4.83	20.41	0.59	2.46	6.73
		Mixer	18.58	4.85	17.14			
	10	Doubler	22.91	5.38	34.67	1.74	6.74	17.14
		Mixer	22.18	5.28	34.67			
	15	Doubler	25.86	5.78	46.06	2.99	11.12	26.36
		Mixer	24.49	5.59	45.33			

The valid restraint region of the mounting configuration with the convex error shown in Fig. 8 and Fig. 9 is only the central part of the support stripe and the tabletting as well as the small screws, so the surface profile exhibits an 'X' shape. Furthermore, the THG efficiency is very sensitive to the convex error and reduces obviously with the increase of the convex error, as shown in Table 3. Especially, the loss of the THG efficiency is far more than 10% when the convex error is larger than 10 μm and the input intensity is relatively high (i.e., 3~4 GW/cm^2).

3.2.3 Condition of the concave error

Fig. 10 and Fig. 11 show the influence of the mounting configuration with a concave error on the KDP crystals when the departure angle is 45°. And the D_{PV} values, the D_{RMS} values, $\Delta\theta_{ave}$ and the loss of the THG efficiency are reported in Table 4.

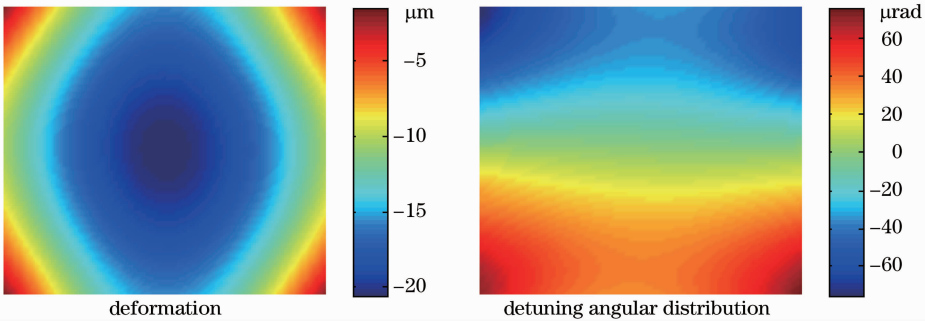

Fig. 10 Deformation and detuning angular distribution of the doubler under concave errors

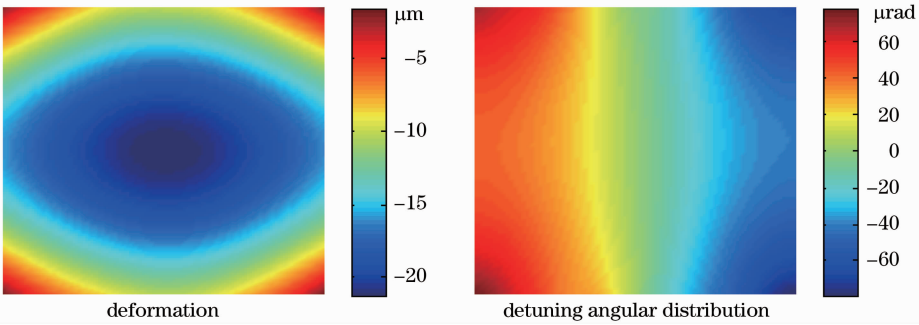

Fig. 11 Deformation and detuning angular distribution of the mixer under concave errors

Table 4 Influence of concave errors on frequency tripling

Departure angle /(°)	Concave error /μm	KDP	D_{PV} /μm	D_{RMS} /μm	$\Delta\theta_{ave}$ /μrad	Loss of the THG efficiency /%		
						2 GW/cm^2	3 GW/cm^2	4 GW/cm^2
30	5	Doubler	11.92	2.75	14.66	0.34	1.32	3.61
		Mixer	12.17	2.81	15.89			
	10	Doubler	15.50	3.20	31.13	1.46	5.52	14.26
		Mixer	15.94	3.31	31.84			
	15	Doubler	18.92	3.88	47.60	3.29	11.85	27.66
		Mixer	20.21	4.11	47.59			
45	5	Doubler	15.41	3.80	14.07	0.32	1.23	3.38
		Mixer	15.81	3.89	15.70			
	10	Doubler	18.99	4.10	30.66	1.43	5.38	13.92
		Mixer	19.58	4.26	31.83			
	15	Doubler	22.54	4.64	47.18	3.26	11.71	27.31
		Mixer	23.77	4.92	47.62			
60	5	Doubler	18.10	4.63	13.64	0.31	1.17	3.23
		Mixer	18.64	4.76	15.53			
	10	Doubler	21.62	4.84	30.41	1.42	5.33	13.76
		Mixer	22.39	5.05	31.84			
	15	Doubler	25.23	5.29	46.85	3.23	11.58	27.03
		Mixer	26.48	5.62	47.66			

Because of the mounting configuration with the concave error, the restraint on the KDP crystals is equivalent to the four corner supports and the surface profile exhibits an elliptical shape, as shown in Fig. 10 and Fig. 11. Meanwhile, the relationship between the concave error and the loss of the THG efficiency is similar to the case of the convex error. Similarly, the loss of the THG efficiency is also very severe when the input intensity is larger than 3 GW/cm^2.

From the above numerical analysis, we can draw some conclusions. Firstly, the influence of the random error on the frequency tripling is the lowest and the frequency tripling can be always efficient even if the random error is up to 15 μm, whereas the convex error and the concave error would cause a larger loss of the THG efficiency. It implies that the peaks of fabrication errors are intensively distributed in certain peripheral regions that make the THG efficiency reduced much more seriously. Secondly, the loss of the THG efficiency is closely related to the input intensity of the fundamental light. Furthermore, the higher input intensity, the larger loss would happen. For example, for the same fabrication error, the maximal loss of the THG efficiency is less than 3.5% when the input intensity is 2 GW/cm^2 and it is up to 27.7% when the input intensity is 4 GW/cm^2. The reason is that the second harmonic conversion efficiency should be 66.7% in order to achieve the maximal THG efficiency for the frequency tripling, and the frequency doubling is very sensitive to the detuning angular distribution for a higher intensity of the fundamental light. Consequently, the variation of the second harmonic conversion efficiency is much larger and it would cause the larger loss of the THG efficiency for the higher input intensity under the same condition of the detuning angular distribution. Thirdly, the THG efficiency is sensitive to the size of fabrication errors and reduces obviously with the increase of fabrication errors, especially the convex error and the concave error. Fourthly, the loss of the THG efficiency increases with the departure angle under the condition of the same input intensity and fabrication error, except the case of the mounting configuration with the concave error. We consider that the restraint of the mounting configuration with the concave error on the KDP crystals is equivalent to the four corner supports, making in the influence of the gravitational sag on the KDP crystals more significant and the surface profile in the central part of the KDP crystals along the extraordinary axis smoother with a larger departure angle.

4 Conclusion

A mounting configuration has been presented in this paper. The KDP crystals are held by their two vertical edges which are parallel to the extraordinary axis with the supporting stripes and the tablettings. According to the analysis results, this new mounting configuration could make the frequency tripling with an efficient conversion. Meanwhile, the influence of fabrication errors on the THG efficiency has been discussed. The loss of the THG efficiency due to fabrication errors is closely related to the input intensity and becomes aggravated with the higher input intensity. Furthermore, the requirements of the peripheral milling have been presented and it would be very helpful to the practical machining process. The mounting configuration with the random error is acceptable, but the tolerance of the convex error and the concave error should be controlled below 5 μm.

Acknowledgments The authors thank Dr. Su Ruifeng (Harbin Institute of Technology) for many fruitful discussions in the finite element models.

Reference

1 P J Wegner, M A Henesian, D R Speck, *et al*.. Harmonic conversion of large-aperture 1.05-μm laser beams for inertial-confinement fusion research[J]. Appl Opt, 1992, 31(30): 6414－6426.

2 Lin Zunqi. Progress of laser fusion[J]. Chinese J Lasers, 2010, 37(9): 2202－2207.
林尊琪. 激光核聚变的发展[J]. 中国激光, 2010, 37(9): 2202－2207.

3 Wang Wenyi, Zhao Runchang, Su Jingqin, *et al*.. Preliminary laser-pulse-shaping experiment on technical integration line[J]. Acta Optica Sinica, 2010, 30(4): 1051－1054.
王文义, 赵润昌, 粟敬钦, 等. 神光Ⅲ原型装置初步的激光脉冲整形实验[J]. 光学学报, 2010, 30(4): 1051－1054.

4 C A Haynam, P J Wegner, J M Auerbach, *et al*.. National Ignition Facility laser performance status[J]. Appl Opt, 2007, 46(16): 3276－3303.

5 H M George, I M Edward, R W Craig. The National Ignition Facility[J]. Opt Eng, 2004, 43(12): 2841－2843.

6 E I Moses, R E Bonanno, C A Haynam, *et al*.. The National Ignition Facility: path to ignition in the laboratory[J]. Eur Phys J D, 2007, 44(2): 215－218.

7 M L Spaeth, K R Manes, C C Widmayer, *et al*.. National Ignition Facility wavefront requirements and optical architecture[J]. Opt Eng, 2004, 43(12): 2854－2857.

8 Dai Wanjun, Zhang Kun, Zhang Xin, *et al*.. Entire beam wavefront measurement in prototype of SG-Ⅲ facility[J]. Chinese J Lasers, 2011, 38(2): 0202007.
代万俊, 张　崑, 张　鑫, 等. 神光-Ⅲ原型装置全光路系统波前测量方法[J]. 中国激光, 2011, 38(2): 0202007.

9 J M Auerbach, C E Barker, S A Couture, *et al*.. Modeling of frequency doubling and tripling with converter refractive index spatial non-uniformities due to gravitational sag[C]. SPIE, 1999, 3492: 472－474.

10 L Olivier, G Claude. Modeling of the effects of KDP crystals gravity sag on third harmonic generation[C]. SPIE, 1999, 3492: 802－808.

11 Jia Kai, Yuan Xiaodong, Xu Xu, *et al*.. Influence of clamping modes in KDP crystal on conversion efficiency of third harmonic generation[J]. High Power Laser and Particle Beams, 2011, 23(6): 1553－1558.
贾　凯, 袁晓东, 徐　旭, 等. 夹持方式对KDP晶体三倍频转换效率的影响[J]. 强激光与粒子束, 2011, 23(6): 1553－1558.

12 S Moaveni. Finite Element Analysis: Theory and Application with

ANSYS[M]. London: Prentice Hall PTR Upper Saddle River, 1999. 168－231.

13 P W Milonni, J M Auerbach, D Eimerl. Frequency conversion modeling with spatially and temporally varying beams[C]. SPIE, 1997, 2633: 230－241.

14 Y Altintas, D Montgomery, E Budak. Dynamic peripheral milling of flexible structures[J]. J Engineering for Industry, 1992, 114(2): 137－145.

15 M Wan, W H Zhang, K P Qiu. Numerical prediction of static form errors in peripheral milling of thin-walled workpieces with irregular meshes[J]. J Manufacturing Science and Engineering, 2005, 127(1): 13－22.

栏目编辑：韩　峰